Electronic structure of nanoscale iron oxide particles measured by scanning tunneling and photoelectron spectroscopies

M. Preisinger,[1] M. Krispin,[1] T. Rudolf,[1] S. Horn,[1] and D. R. Strongin[2]
[1]*Institute of Physics, University of Augsburg, 86135 Augsburg, Germany*
[2]*Department of Chemistry, Temple University, Philadelphia, Pennsylvania 19122, USA*
(Received 6 December 2004; published 7 April 2005)

We have investigated the electronic structure of nanosized iron oxide by scanning tunneling microscopy and spectroscopy as well as by photoelectron spectroscopy. The nanoparticles were produced by the thermal treatment of ferritin molecules containing a self-assembled core of iron oxide. Depending on the thermal treatment we were able to prepare different phases of iron oxide nanoparticles resembling γ-Fe_2O_3, α-Fe_2O_3, and a phase which apparently contains both γ-Fe_2O_3 and α-Fe_2O_3. The changes to the electronic structure of these materials were studied under reducing conditions. We show that the surface band gap of the electronic excitation spectrum can differ from that of bulk material and is dominated by surface effects.

DOI: 10.1103/PhysRevB.71.165409 PACS number(s): 73.22.−f, 79.60.Jv, 68.37.Ef, 81.07.−b

I. INTRODUCTION

Nanosized transition metal oxide particles can be expected to show size-dependent optical, magnetic, and chemical properties with possible applications in catalysis and magnetic and optical devices. It has already been shown that catalytic and magnetic properties of nanoparticles might be quite different from bulk materials. An example are nanosized particles of the compound Fe_2O_3, which exhibit superparamagnetism,[1–3] and, at the same time, enhanced catalytic properties, compared to the bulk material.[4] The size dependence of the catalytic properties can be associated with an influence of size on the electronic structure of the material. This influence can be due to the surface tension of the particle, resulting in an effective pressure or to changes in the stoichiometry (and resulting changes of the state of oxidation of Fe) of such particles, driven by the large surface-to-volume ratio.

Here we investigate the electronic structure of nanosized iron oxide by scanning tunneling microscopy and spectroscopy as well as by photoelectron spectroscopy and optical spectroscopy. To address the question of stoichiometry and oxidation state the effect of the oxidizing and reducing atmosphere on the electronic structure of the nanoparticles is also investigated. To produce nanosized iron oxide particles we utilized the ability of ferritin to self-assemble and construct a core of iron oxide. ferritin is the major cellular iron-storage protein, and it consists of a spherical hollow shell composed of 24 polypeptide subunits. It is able to store iron as hydrated iron oxide in the internal cavity.[5–7] The inner and outer diameters of the protein shell are about 8 and 12.5 nm, respectively. The iron core shows a structure similar to that of the mineral ferrihydrite ($5Fe_2O_3 \cdot 9H_2O$). Hydrophilic and hydrophobic channels penetrate the protein shell and provide the means by which iron and other atoms can be accumulated within or removed from the molecules. In previous work, ferritin was used to prepare several kinds of nanoparticles and nanocomposites.[8,9] Furthermore, ferritin molecules inherently show photocatalytic activity.[10]

II. EXPERIMENTAL SECTION

Monolayers of ferritin molecules were prepared by the Langmuir-Schaefer technique.[11] A ferritin solution (0.15 mg/ml horse spleen ferritin from Sigma) in 10 mM NaCl with a pH of 5.5 was filled in a commercially available Langmuir Trough (Nima Technology). A few micrograms of trimethyloctadecylammonium bromide (Fluka) were dissolved in chloroform to form a concentration of 1 mg/ml and was then spread over the ferritin solution subphase. After compression to a surface pressure of 30 mN/m and an adsorption time of a few minutes the monolayer was transferred to a freshly cleaved surface of a highly oriented pyrolytic graphite (HOPG) substrate by the horizontal lifting method. Further details of the preparation of two-dimensional (2D) arrays are described elsewhere.[12,13]

Prior to the introduction into the ultrahigh vacuum (UHV) chamber all samples were annealed in air at different temperatures and for different time intervals (~575 K for 1 h, ~675 K for 1 h, or ~675 K for 5 h) to eliminate the protein shell and to further oxidize the iron core. After introduction into the chamber the samples were annealed *in situ* under a 1×10^{-6} mbar oxygen atmosphere at the respective temperature for a few minutes. Utilizing this process we produced dense arrays of iron oxide nanoparticles. To vary the oxidation state of the respective nanoparticles, we reduced the sample within the UHV system by exposure to 1×10^{-6} mbar of a H_2/Ar atmosphere (25% H_2, 75% Ar) at ~675 *K* for 2 h.

Spectroscopic measurements were carried out in an Omicron UHV system, equipped with a DAR400 x-ray radiation source (Al Kα 1486.6 eV) and an AR65 electron analyzer for x-ray photoelectron spectroscopy (XPS). Scanning tunneling microscopy (STM) and spectroscopy (STS) measurements were performed using a variable temperature scanning probe microscope (VT-SPM) within the same UHV system. All STM images were recorded in the constant current mode, using a tungsten tip at a sample bias of −1.5 V and a current of 0.1 nA. The topographic images represent the height $z(x,y)$ of the tunneling tip above the sample after a plane and

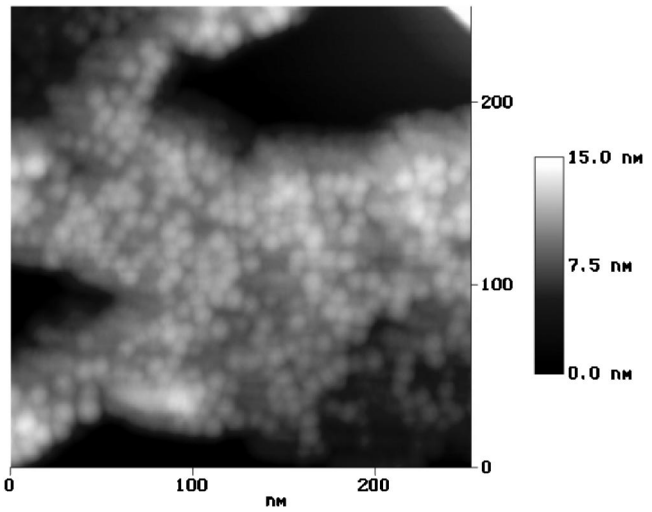

FIG. 1. AFM image taken on a ferritin monolayer without annealing.

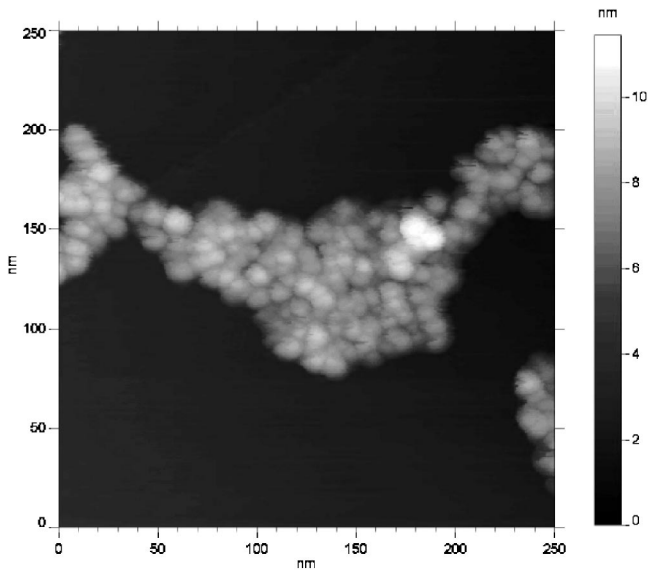

FIG. 2. STM image of an oxidized ferritin monolayer, showing iron oxide nanoparticles.

slope subtraction was performed. The STS measurements were carried out by placing the tunneling tip above a single nanoparticle and keeping the tip-sample separation fixed while recording the $I(U)$ characteristic. A Bruker Fourier-transform infrared spectrometer (FTIR) was used for optical spectroscopy. The STM and STS measurements were done on monolayers of nanoparticles, while the XPS and optical spectroscopy measurements were done on thicker samples in order to improve the signal-to-noise ratio. Such samples were prepared from a small dried drop of ferritin solution (1 mg/ml) annealed in air at the respective temperatures.

III. RESULTS

Images of monolayers of ferritin molecules under air (Fig. 1) were taken by tapping mode atomic force microscopy [(TM-AFM), utilizing a Nanoscope IIIa from Digital Instruments]. The layer of ferritin molecules is not completely closed. The difference in height between the ferritin layer and the subjacent HOPG substrate of about 10 nm corresponds to the thickness of a single ferritin monolayer. Also the diameter of the spheres observed is approximately 10 nm, which is characteristic of ferritin molecules with a dehydrated protein shell caused by drying under air.

Depending on the oxidation parameters, we obtain nanoparticles of different iron oxide phases. X-ray diffraction (XRD) performed on a thick layer of ferritin annealed at ~675 K under air for 1 h (procedure 1) reveals rather broad reflections characteristic of γ-Fe_2O_3 with some contributions of α-Fe_2O_3. In the following we will refer to this mixed phase as χ-Fe_2O_3. Further annealing for 5 h (procedure 2) resulted in the narrow reflections characteristic of α-Fe_2O_3. These results are consistent with transmission electron microscopy (TEM) studies, which will be described elsewhere.[14] Annealing ferritin molecules at ~575 K in air (procedure 3) results in γ-Fe_2O_3 nanoparticles, as confirmed by TEM.

A STM image of an nanoparticle monolayer after annealing in air (procedure 1) is shown in Fig. 2. Here we note that the images of the nanoparticles of all three phases (not shown) look alike. The image shows densely packed clusters of distinguishable nanoparticles. After the annealing process the removal of the protein shell results in a lower coverage of the HOPG surface. The nanoparticle clusters consist of well defined particles of a size of approximately 7–8 nm. Such a size is expected for the iron oxide core of ferritin. Clusters are found predominantly at steps present on the HOPG substrate surface.

To obtain information concerning the iron oxidation state we performed XPS on the nanoparticles. Figure 3 displays the Fe $2p$ XPS spectra characteristic of the oxidized nanoparticle phases and, for comparison, the spectra of Fe_2O_3 and FeO, taken from bulklike material.[15,16] The latter two spectra correspond to an Fe^{3+} and an Fe^{2+} state, respectively. We did not observe any charging effects of the nanoparticles within the instrumental width of about 0.2 eV. With respect to the

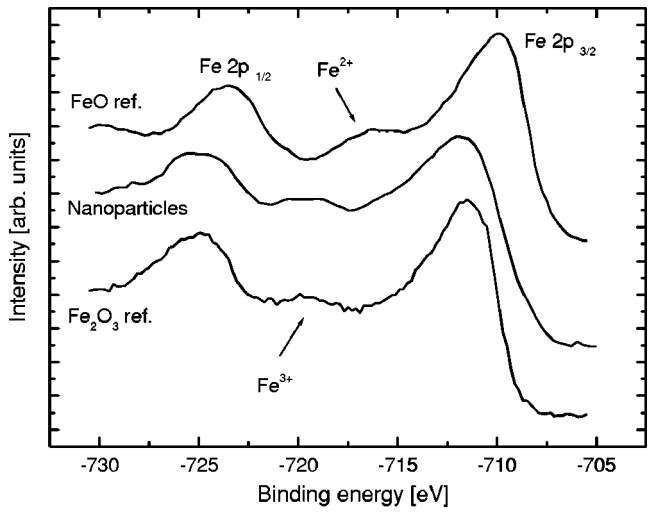

FIG. 3. XPS spectra of oxidized ferritin molecules (Fe_2O_3 nanoparticles) and reference data of bulklike samples.

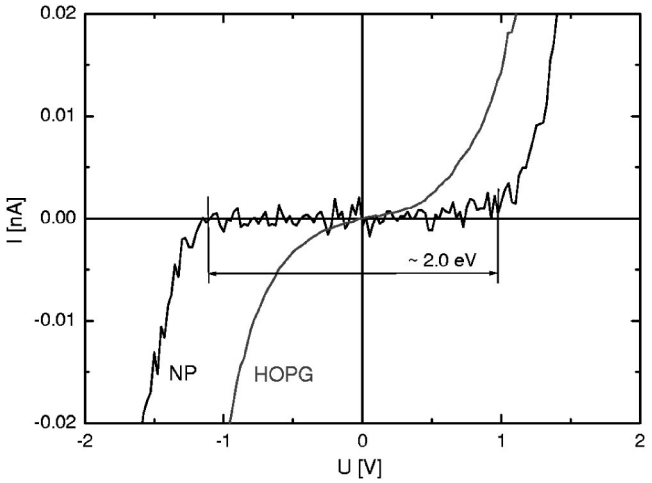

FIG. 4. STS spectra of α-Fe_2O_3 nanoparticles compared to the HOPG substrate.

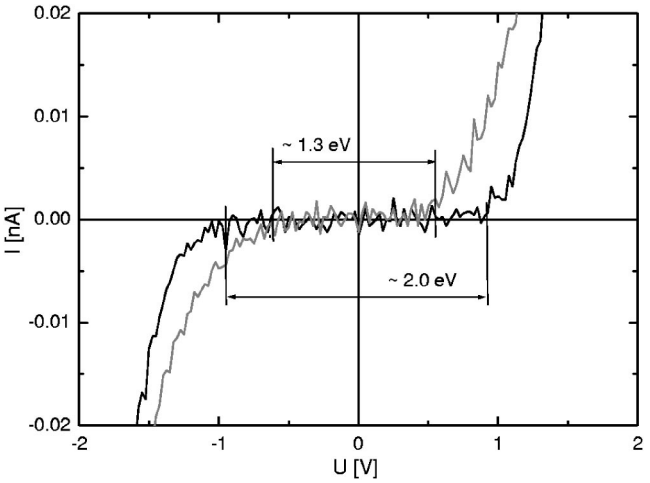

FIG. 5. STS spectra of γ-Fe_2O_3 nanoparticles.

Fe^{2+} spectrum, the Fe^{3+} spectrum is shifted to a higher binding energy by 1.5 eV, and it shows a characteristic satellite structure at a binding energy E_b=719 eV. The Fe^{2+} spectrum shows a satellite structure at E_b=716 eV. An Fe $2p_{3/2}$ peak at 711.7 eV and a satellite structure at about 719 eV in the spectrum taken from the iron oxide nanoparticles is characteristic for an Fe^{3+} state, although the presence of a slight weight of Fe^{2+} cannot be ruled out. Further oxidation of the particles within the UHV system at an oxygen partial pressure of 1×10^{-6} mbar and a temperature of ~675 K does not result in changes of the intensity of the characteristic satellite, nor did it shift the spectrum to higher binding energies. We, therefore, conclude that either (i) the Fe atoms of the nanoparticles are already in the highest oxidation state (Fe_2O_3), or (ii) the Fe atoms are not in the highest oxidation state, but further oxidation of the nanoparticles is not possible under the chosen conditions.

To investigate the electronic excitation spectrum of single nanoparticles in the vicinity of the Fermi energy E_F, STS measurements were performed on the three different phases identified by XRD and TEM (α-Fe_2O_3,γ-Fe_2O_3,χ-Fe_2O_3). It is well known, that tunneling spectra obtained from nanocrystals may depend on the tunneling parameters and tunneling configuration due to, e.g., charging,[17,18] rendering the determined gap width unreliable. Therefore we adjusted the tunneling parameters to perform the measurements at a large tunneling tip-nanoparticle distance. The distance was increased until a constant gap value was observed and charging effects did not occur.

A typical tunneling spectrum taken from a single α-Fe_2O_3 nanoparticle (NP) is plotted in Fig. 4. For comparison, a spectrum taken from the HOPG substrate is also shown. The $I(U)$ curves taken from the nanoparticle clearly are characteristic for a gap energy of Δ=2.0 eV. The variation in the gap energy for spectra taken from the same nanoparticle was within the error of the measurement. Spectra were taken from a few tens of different nanoparticles, and the gap energy was found to vary between 1.8 and 2.2 eV. This variation might reflect differences in particle size, surface conditions, and small variations of the tunneling junction parameters for the different measurements. The gap energy of Δ=2.0 eV corresponds to that measured on a bulk α-Fe_2O_3 sample (Δ=2.2 eV).[7] Figure 5 displays tunneling spectra taken off γ-Fe_2O_3 nanoparticles. Here, spectra taken from different locations of a single nanoparticle show two different values of the gap energies, Δ_1=1.3 eV (±0.2 eV) and Δ_2=2.0 eV (±0.2 eV). We note that the gap energy of a bulk sample of γ-Fe_2O_3 shows a gap of 2.0 eV.[7] Finally, tunneling spectra taken from χ-Fe_2O_3-phase nanoparticles show a band gap of 1.3 eV (±0.2 eV) (Fig. 6), which does not change for different locations on one nanoparticle. A gap value of 1.3 eV does not correspond to the gap energy of any bulk iron oxide phase.[7]

Keeping in mind that STS is a highly surface-sensitive technique, we carried out optical spectroscopy on nanoparticles of the χ-Fe_2O_3 phase in order to obtain information corresponding to "bulk properties." Figure 7 shows the optical transmission data taken from a thick layer of such particles. The spectrum displays a strong decrease of transmission at around 2.0 eV, and a less pronounced decrease at about 1.3 eV. These energies agree well with the two different gap energies inferred from STS measurements on such

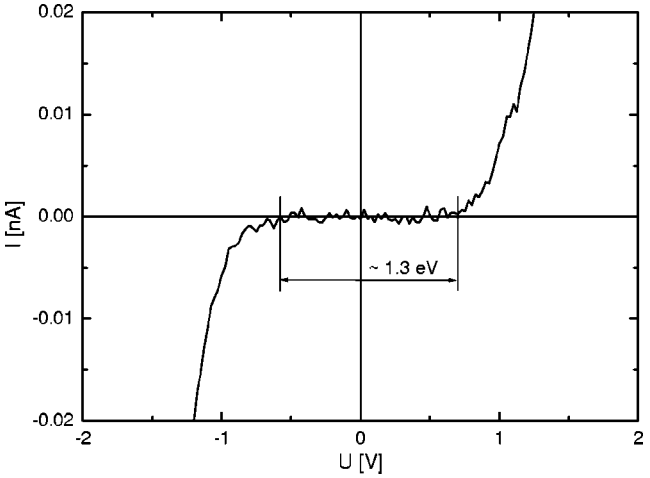

FIG. 6. STS spectra of χ-Fe_2O_3 nanoparticles.

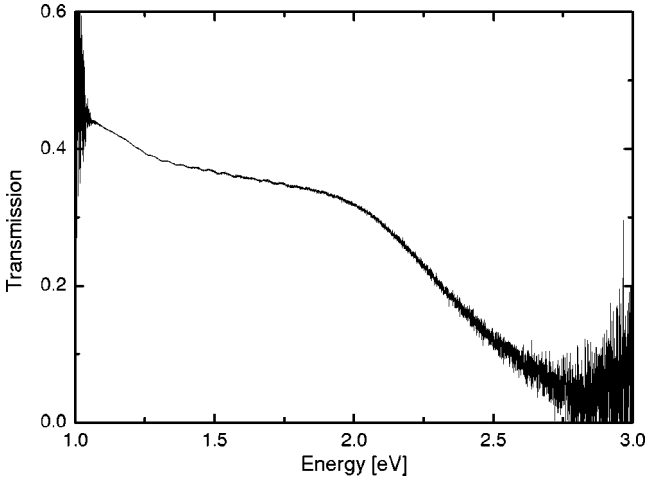

FIG. 7. Optical transmission of χ-Fe_2O_3 nanoparticles.

particles. In a straightforward interpretation we assign the feature at 2 eV to the bulk gap and the feature at 1.3 eV to a surface gap. This interpretation will be discussed in more detail below.

An interesting question concerns the possibility of manipulating the electronic properties of the nanoparticles. To this end we exposed χ-Fe_2O_3 nanoparticles *in situ* at a temperature of $\sim$675 K to a reducing H_2/Ar atmosphere of 1×10^{-6} mbar (25% H_2, 75% Ar) for 2 h. Figure 8 compares the Fe 2*p* spectrum of the nanoparticles before and after reduction. As is clearly seen, the spectrum of the reduced sample is shifted to lower binding energies by about 1.2 eV compared to the spectrum before reduction. In addition, an Fe^{2+} satellite structure develops, marked by an arrow in Fig. 8.

STM imaging shows (Fig. 9) that the shape and size of the nanoparticles are not changed by the reduction process. From the STS measurements we infer, within the margins of error, the same gap of 1.3 eV (±0.2 eV) as before the reduction (Fig. 10).

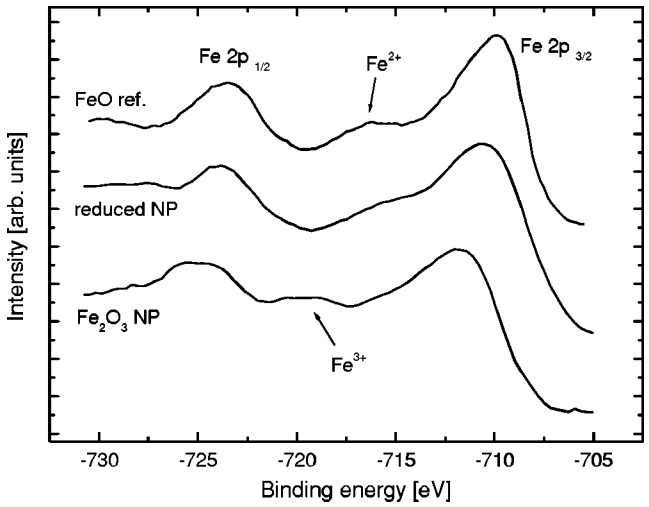

FIG. 8. XPS spectra of oxidized and reduced iron oxide nanoparticles compared to FeO reference data.

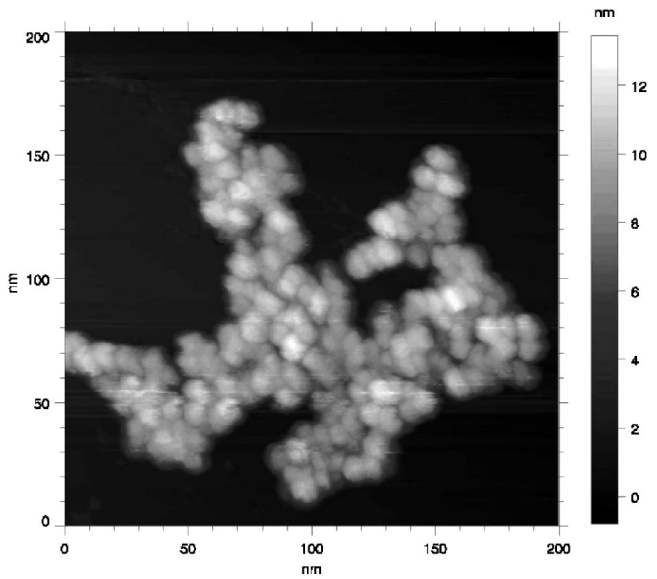

FIG. 9. STM image of the reduced χ-Fe_2O_3 nanoparticles.

IV. DISCUSSION

We first address the question of the valence of the iron ions in the nanoparticles. From the Fe 2*p* binding energy and the position and intensity of the corresponding satellite structure as measured by XPS we conclude that the iron valence state of the oxidized samples is Fe^{3+}. This is in agreement with expectations, since it is well known that ferrihydrites transform into α- or γ-Fe_2O_3 at 573–723 K under air.[7] Further evidence for an Fe^{3+} state after annealing under air comes from XRD and TEM,[14] which show the nanoparticles to consist of different phases of Fe_2O_3, depending on the oxidation procedure. Bulk Fe_2O_3 is an insulator with a gap of $\Delta=2.0$ eV for the γ-phase and $\Delta=2.2$ eV for the α-phase. The gap energy obtained for the α-phase nanoparticles by STS is consistent with that for the bulk material. The γ-Fe_2O_3-phase nanoparticles show a band gap of 1.3 eV or 2.0 eV, depending on the location of the tunneling tip on the

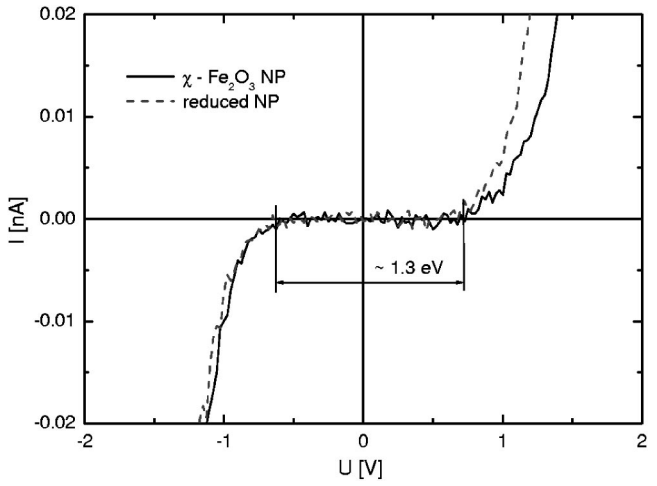

FIG. 10. STS spectra of oxidized and reduced iron oxide nanoparticles.

same particle. This suggests two different types of phases within one nanoparticle. The fact that bulk γ-Fe_2O_3 has a band gap of 2.0 eV (Ref. 7) suggests that it is one of these phases. From single crystal studies it is known that γ-Fe_2O_3 crystallizes in an iron-deficient structure similar to the inverse spinel structure of Fe_3O_4 ($A[BA]O_4$, $A=Fe^{3+}$, $B=Fe^{2+}$), but in γ-Fe_2O_3 there are randomly distributed cation vacancies on the B site. Such a defect-rich structure might be subject to reconstruction effects, especially at the surface of a nanoparticle or by impurity atoms such as, e.g., carbon introduced by the original organic shell of the particle. Such a reconstructed phase can yield a different gap than the bulk. The XPS and FTIR measurements might be affected by such surface effects in a much lesser degree because of their lower surface sensitivity. This will be discussed in more detail below.

The FTIR spectrum taken from the χ-Fe_2O_3 phase sheds further light on the origin of the 1.3 eV gap. Two significant features were identified in this spectrum, one of which coincides with the gap of 1.3 eV found by STS. From the fact that the slope of the absorption coefficient is much smaller at 1.3 than at 2 eV, but that the surface sensitive STS measurements detect only one gap at 1.3 eV, we conclude that the 1.3 eV gap is a property of the surface of the nanoparticle, most likely due to a surface reconstruction. The bulk of the nanoparticle then exhibits the gap expected from the bulk γ- or α-Fe_2O_3. It is striking that a surface reconstruction would only occur in the γ-Fe_2O_3 and χ-Fe_2O_3 nanoparticles. The reason for this could be attributed to the defect-rich nature of these phases.

The interpretation of the 1.3 eV gap as a surface effect is further corroborated by our reduction experiments. There are several studies concerning the reduction of iron oxides. For example, α-Fe_2O_3 can be reduced to metallic iron via a series of intermediate oxides, like Fe_3O_4 and FeO.[19] As shown above we achieved a significant reduction of the χ-Fe_2O_3 nanoparticles by annealing in an H_2/Ar atmosphere, as evidenced by XPS measurements. The resulting XPS spectrum is compatible to an FeO reference spectrum taken from a macroscopic sample. However, a stable cation-deficient phase of FeO exists at ambient pressure only at temperatures above 840 K. This nonstoichiometric form of FeO can be obtained as a metastable phase at room temperature by rapid quenching.[7] Although we cannot expect a stable FeO bulk phase from the applied annealing procedure under ambient conditions, we cannot exclude that the FeO phase is stabilized under UHV due to its nanocrystalline form. This conclusion is supported by former studies on epitaxial films showing that the stabilization of an FeO phase depends on film thickness.[15,20,21]

Interestingly, a change of the iron oxidation state under reducing conditions, as reflected in the XPS measurements, does not affect the energy gap of the nanoparticles as measured by STS. Taking into account the probing depth of XPS at the Fe 2p binding energy we conclude that about 40% of the volume of a particle contributes to the XPS spectrum, while contributions to the STS measurements originate from a surface layer of the particle, which amounts to only 10% of its volume. Obviously, for nanoparticles XPS is far more bulk sensitive than STS. Therefore, we attribute the independence of the gap value upon iron reduction to the fact that the gap value measured by STS is dominated by the surface structure of the nanoparticle. This surface structure appears to be unaffected by reduction. This finding is consistent with our conclusion above that the 1.3 eV band gap of χ-Fe_2O_3 is due to surface effects.

In conclusion, only nanoparticles of the thermodynamically stable α-Fe_2O_3 phase show a band gap compatible to the bulk material in surface-sensitive STS measurements. The STS measurements on all other nanoparticle phases investigated (γ-Fe_2O_3, χ-Fe_2O_3, and FeO) demonstrate the existence of a surface band gap of 1.3 eV, although volume-sensitive measurements reveal a band gap compatible with the bulk material. We therefore conclude that the band gap does not depend on the size of the nanoparticles for diameters above 8 nm, but that properties, such as, e.g., the photocatalytic activity of such particles, are due to the formation of a surface band gap different from that of the volume. The existence of such a surface band gap appears to be triggered by defects within the nanoparticle.

ACKNOWLEDGMENT

This work was supported by the Deutsche Forschungsgemeinschaft through SFB 484.

[1] A. E. Berkowitz, W. J. Schuele, and P. F. Flanders, J. Appl. Phys. **39**, 1261 (1968).
[2] C. Janzen, J. Knipping, B. Rellinghaus, and P. Roth, J. Nanopart. Res. **5**, 589 (2003).
[3] T. P. Raming, A. J. A. Winnubst, C. M. van Kats, and A. P. Philipse, J. Colloid Interface Sci. **249**, 346 (2002).
[4] P. Li, D. E. Miser, S. Rabiei, R. T. Yadav, and M. R. Hajaligol, Appl. Catal., B **43**, 151 (2003).
[5] S. Mann, J. Webb, and R. J. P. Williams, *Biomineralization* (VCH, Weinheim, 1989).
[6] W. H. Massover, Micron **24**, 389 (1993).
[7] R. M. Cornell and U. Schwertmann, *The Iron Oxides* (VCH, Weinheim, 1996).
[8] K. K. W. Wong and S. Mann, Adv. Mater. (Weinheim, Ger.) **8**, 928 (1996).
[9] H. A. Hosein, D. R. Strongin, M. Allen, and T. Douglas, Langmuir **20**, 10 283 (2004).
[10] I. Kim, H. A. Hosein, D. R. Strongin, and T. Douglas, Chem. Mater. **14**, 4874 (2002).
[11] G. G. Roberts, *Langmuir-Blodgett Films* (Plenum, New York, 1990).
[12] C. A. Johnson, Y. Yuan, and A. M. Lenhoff, J. Colloid Interface Sci. **233**, 261 (2000).
[13] T. Furuno, H. Sasabe, and K. M. Ulmer, Thin Solid Films **180**, 23

(1989).
[14] K. Bremser, Diploma thesis, University of Augsburg, 2004.
[15] W. Weiss and W. Ranke, Prog. Surf. Sci. **70**, 1 (2002).
[16] M. Oku, K. Wagatsuma, and T. Konishi, J. Electron Spectrosc. Relat. Phenom. **98–99**, 277 (1999).
[17] E. P. A. M. Bakkers and D. Vanmaekelbergh, Phys. Rev. B **62**, R7743 (2000).
[18] D. Katz, O. Millo, S. Kan, and U. Banin, Appl. Phys. Lett. **79**, 117 (2001).
[19] M. Rau, D. Rieck, and J. W. Evans, Metall. Trans. B **18**, 257 (1987).
[20] A. N. Koveshnikov, R. H. Madjoe, J. Karunamuni, R. L. Stockbauer, and R. L. Kurtz, J. Appl. Phys. **87**, 5929 (2000).
[21] G. Ketteler and W. Ranke, J. Phys. Chem. B **107**, 4320 (2003).